MODELING FIRES IN ADJACENT SHIP COMPARTMENTS WITH COMPUTATIONAL FLUID DYNAMICS

S. D. Wix, J. K. Cole, and J. A. Koski

Sandia National Laboratories, PO Box 5800, Albuquerque, NM 87185-0525

SUMMARY

This paper presents an analysis of the thermal effects on radioactive (RAM) transportation packages with a fire in an adjacent compartment. An assumption for this analysis is that the adjacent hold fire is some sort of engine room fire. Computational fluid dynamics (CFD) analysis tools were used to perform the analysis in order to include convective heat transfer effects. The analysis results were compared to experimental data gathered in a series of tests on the United States Coast Guard ship Mayo Lykes located at Mobile, Alabama.

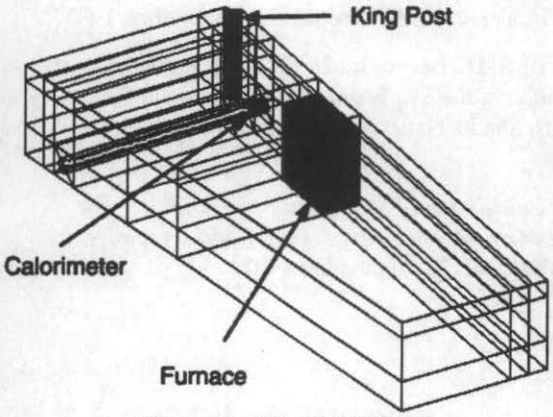

Figure 1 - Ship Hold Model

INTRODUCTION

Transport of radioactive or other hazardous materials by sea requires care to ensure that the protective package guards against potential hazards. Shipboard fires are one threat that must be carefully considered to assure safe arrival at the final destination. A possible scenario is of a ship fire breaking out in an adjacent compartment, such as an engine room, to the cargo hold. This paper presents an analysis of the thermal effects on radioactive (RAM) transportation packages with a fire in an adjacent compartment.

To assure that others interested in the problem can apply the results of this paper, a commercially available computational fluid dynamics (CFD) computer code, CFX, marketed by AEA Technologies has been used. This code was selected because of its previous use in fire analyses, and its ability to treat all heat transfer mechanisms, i.e., conduction, convection and thermal radiation, in a coupled manner. In addition, an effort has been made to limit the input of experimental results into the analysis model so that analysts without access to the detailed experimental data can confidently create similar models.

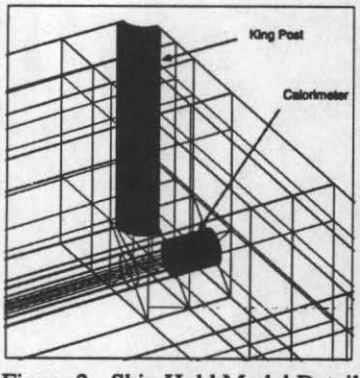

Figure 2 - Ship Hold Model Detail

SHIP HOLD MODEL DESCRIPTION

The CFD model of the ship hold is a three-dimensional sym-

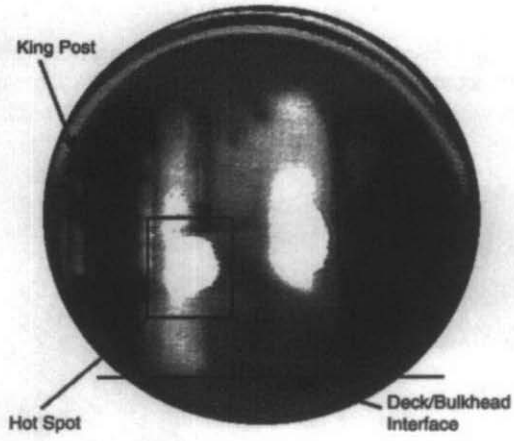

Figure 3 - Bulkhead IR Image

metric model and contains 64,352 cells. An axis of symmetry at the ship centerline was used to reduce the overall size of the model. Heat conducting solids were used to include the thermal capacitance of features such as the hold bulkheads, deck and overhead, the calorimeter and the king post. A weakly compressible buoyancy model, which means only density is a function of temperature, was used since any flow will be induced by natural convection. The model also used the k-e turbulent flow formulation for calculating fluid flow. Figure 1 presents the overall ship hold CFD model and Figure 2 presents a detail of the model.

A radiation heat transfer model of the ship hold was also constructed to run simultaneously with the flow solver. The CFD model and the radiation model are coupled automatically to produce the interaction between convective, conductive and radiative heat transfer. The CFD model transfers either temperatures or heat fluxes to the radiation model, depending on the type of wall boundary condition. The radiation model then solves the radiation problem by tracking photons through a set of zones that form the calculation domain, i.e., the radiation model, and returns either heat fluxes or temperatures to the CFD model. The radiation model software can use either a Monte Carlo method or a discrete transfer, or Shaw method, for solving the radiation heat transfer problem. For this simulation, the Shaw method was used. The radiative emmisivity of the bulkheads, deck, and overhead was 0.75 and the radiative emmisivity of the calorimeter was 0.8. All surfaces except the axis of symmetry wall, had a surface roughness, which is the fraction of reflection which is diffuse, of 1.0. For the axis of symmetry wall, the albedo was 1.0, which means that the axis of symmetry wall was assumed to be a perfect reflective surface. A grey body assumption was used in the radiation model and the media within the model was nonparticipating.

The bulkheads of the Mayo Lykes were 0.008 m thick, the deck and overhead were 0.011 m thick, and the hull was 0.018 m thick. These features were modeled using heat conducting solid elements. A king post was present in the hold and was also modeled using heat conducting solids.

The materials used for this analysis are air and mild steel. The thermal properties of air are temperature-dependent. The mild steel thermal properties were constant and the values of thermal conductivity, density and specific heat are 45 W/m-°C, 7849.8 kg/m3, and 460 J/kg-°C, respectively.

For the Sandia ship fire test experimental program, an instrumented Schedule 60 carbon steel pipe calorimeter with a nominal diameter of 2 feet (0.61 m), a wall thickness of 2.5 cm and a length of 1.5 m was used to measure heat fluxes and temperatures. The cylindrical shape is typical of many radioactive material packaging. The calorimeter midpoint was positioned at the centerline of the ship during the ship fire tests. Half the calorimeter was included in the ship hold model for comparing experimental and calculated results, and positioned at the same location as the calorimeter in the fire tests.

BOUNDARY CONDITIONS

This analysis is a simulation of a ship hold thermal response with a fire in an adjacent hold. An underlying assumption of this analysis is the adjacent hold is the ship engine room. The flame of the engine room fire is assumed to be in contact with the hold bulkhead and creates a localized hot spot on the bulkhead. The size and shape of the hot spot used in the analysis was taken from the experimental portion of the Sandia ship fire test program. Infrared images of the bulkhead were taken during the experimental heptane spray tests and the size of the hot spot was scaled from the infrared image. Figure 3 presents the IR image. The features visible in the IR image are the king post, the hot spot, and the intersection of the hold bulkhead and deck. Since the king post diameter and the deck/bulkhead intersection were known, it was possible to determine an approximate size and location of the hot spot on the bulkhead. The hot spot was connected via radiation and convection to a boundary condition node set at 900°C, which is in the expected range of flame temperatures. A flame emmisivity of 0.9 and a convection coefficient of 10 W/m^2-°C was used.

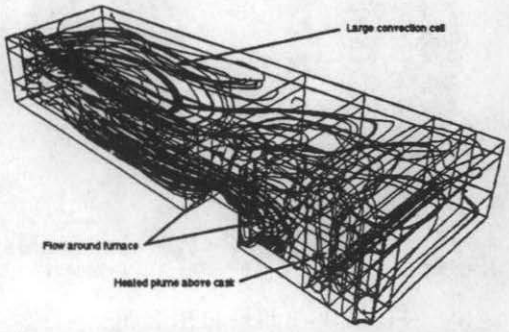

Figure 5 - Four Nozzle Streamline Flow Pattern at 60 Minutes

Two distinct sets of boundary conditions were applied to the ship hold model. The boundary conditions were based on the Sandia ship fire test program experiments. The first set of boundary conditions is named two nozzle boundary condition. The experimental two nozzle boundary condition consisted of a single nozzle directing flames on the ship hold bulkhead on either side of the ship centerline. The second set of boundary conditions is named four nozzle boundary conditions and is based on the experiment using two nozzles directing flames on either side of the ship centerline.

A symmetry wall was used to model the axis of symmetry in the hold. The symmetry wall had a shear stress of zero to reflect the axis of symmetry in the flow field. By using a shear stress of zero at the axis of symmetry, the no-slip wall boundary condition was avoided and the flow in the plane of the symmetry wall was not influenced by the symmetry wall

Natural convection boundary conditions were assumed on the exterior of the hold. A convection coefficient was calculated depending upon orientation. For the bulkheads, the convection coefficient was 4.63 W/m^2. For the deck and overhead, the convective coefficients were 0.775 W/m^2 and 5.67 W/m^2, respectively.

The ambient temperature for the two nozzle calculation was 35°C. FOr the four nozzle calculation, the ambient temperature was 15 °C. The ambient temperatures were from the experimental data.

RESULTS

FLOW PATTERNS

Figures 4 presents a streamline plot of the four nozzle adjacent hold thermal simulation. Streamline plots are zero mass particle tracks at a given time in the simulation. The streamline plots are based on a plane seeding of the zero mass particles. The seeding plane is parallel to the x and y axes and slices through the midpoint of the calorimeter.

Figure 4 show the flow pattern for the four nozzle calculation 60 minutes. As in the two nozzle calculation, fluid flow is developing around the furnace. A plume above the calorimeter is also formed, although the plume is not as apparent in the four nozzle calculation. The lower ambient temperature of the four nozzle calculation may contribute to the less prominent plume above the calorimeter. The large convection cell in the rear section of the hold also formed during the four nozzle calculation. The plots also show that the formation of the convection cell is a long term event. The long formation time is an indicator of the relatively minor contribution of convection heat transfer to this problem.

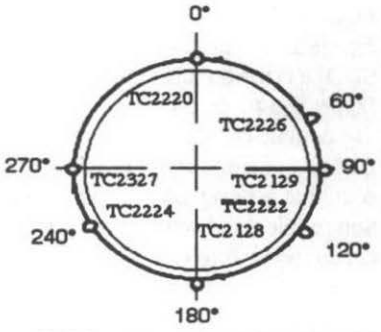

Figure 6 - Experimental and Calculated Temperature Locations on the Calorimeter

SURFACE TEMPERATURE COMPARISON

The analytical and experimental data were compared at seven locations on the calorimeter. Three of the analytical temperature locations (60, 120 and 240 degrees) coincided with experimental thermocouple positions. The remaining four temperature comparisons (0, 90, 180 and 270 degrees) used the average analytical temperature from analytical temperature locations on either side of the experimental thermocouple location. The analytical temperature locations were 4.5 degrees on either side of the experimental thermocouple location. Figure 6 presents the experimental and calculated temperature locations used for data comparison.

Figure 8 is a time-temperature comparison, at 0, 60 and 90 degrees on the calorimeter, for the four nozzle model calculation and experimental data. The peak temperature difference between the experimental and calculated temperatures is 1° C and occurs at 60 degrees on the calorimeter. The calculation temperatures encompass the experimental temperatures with the calculated temperatures at 90 degrees lower that the experimental temperature data at 90 degrees. The temperature distribution indicates that the hot spot area or the hot spot position or some combination of hot spot area and position of the experiment and the calculation was different. The peak temperature occurs at the same time for the calculated and experimental temperature data and is at 65 minutes.

Figures 9 is a circumferential temperature plots at 30 minutes for the four nozzle case. Thirty minutes was chosen as the time because 30 minutes is half way through the experiment and calculation and was chosen to represent a typical circumferential temperature distribution.

The peak calculated temperature for the four nozzle case is higher than the peak experimental

temperature. The temperature distribution of the is comparable between the calculated and experimental temperatures. There is a shift in the location of the maximum and minimum temperature which, again, is probably due forward bulkhead hot spot area and position differences.

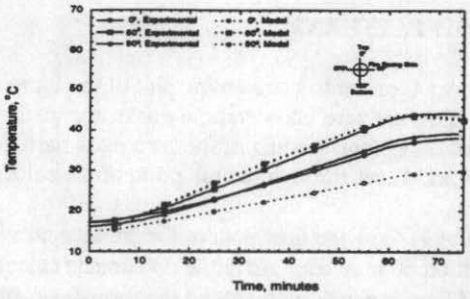

Figure 8 - Four Nozzle Calorimeter Temperature Response at 0, 60 and 90 degrees

HEAT FLUX COMPARISON

Figures 11 and 12 present calculated surface heat flux plots of the calorimeter. SODDIT, the Sandia One Dimensional Direct and Inverse Thermal code was used to calculate the surface heat fluxes. SODDIT is a one dimensional transient thermal code that is designed to solve a wide variety of thermal problems, including inverse heat conduction problems. Inverse heat conduction problems are where interior temperatures are used to calculate the surface heat flux and temperature that caused the interior temperature response. The same code and procedure was used to calculate surface heat fluxes from the experimental data.

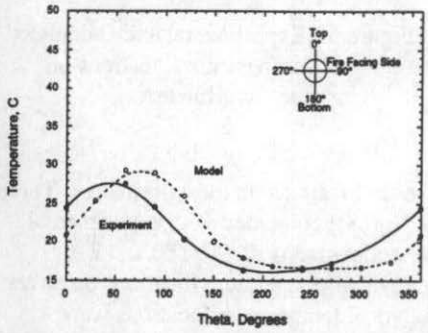

Figure 10 - Four Nozzle Circumferential Calorimeter Temperature Response at 30 Minutes

Figure 12 is the surface heat flux plot the two nozzle case. Again, the heat fluxes are in the range of heat fluxes calculated from the experimental data.

Figure 13 is a circumferential heat flux plot at 30 minutes for the four nozzle case. The heat fluxes are of the same order of magnitude as the experimental data. There is a shift in the maximum and minimum heat flux similar to what was presented in the cirumferential temperature plots. The heat flux positional shift is probably due forward bulkhead hot spot area and position differences.

RADIATION/CONVECTION HEAT TRANSFER PARTITIONING

The CFD model was used to estimate the partitioning of the convection/conduction component of the overall heat transfer mechanism and radiation heat transfer mechanism for the heat transferred to the calorimeter. The partitioning was accomplished by removing buoyancy from the convection model and by the use of a small value of thermal conductivity for the air to minimize conduction. The calculations were made using the same model, boundary conditions and factors such as time step.

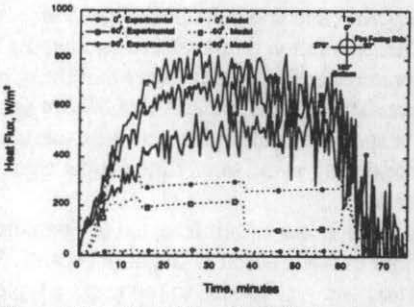

Figure 12 - Four Nozzle Calorimeter Surface Heat Flux

Figure 15 is a comparison of the calorimeter surface temperature with and without convection of, and conduction through the fluid. The plot indicates that convection is a minor contributor to the heat transfer that occurs in this problem since the there is not an appreciable difference between the two sets of temperature data.

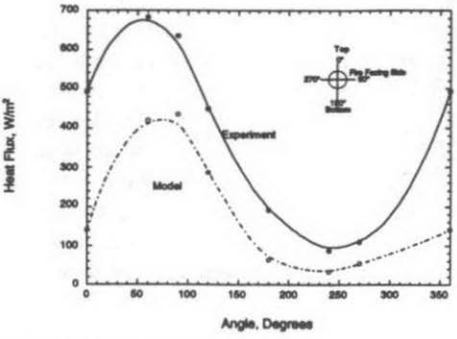

Figure 14 - Four Nozzle Calorimeter Circumferential Surface Heat Flux

However, the plot also shows that convection is present, and for other ship fire problems or other locations in the hold, convection could be more significant. As seen in the streamline plots, there is a large convection cell in the aft part of the hold. If the calorimeter were in the aft part of the hold, convection could have a larger contribution to the overall heat transfer. Another location where convection contributes to the overall heat transfer mechanism is at just aft of the front bulkhead where the hot spots are. The convection driving potential is larger in this area due to the larger temperature difference between the air and heated surface.

SHADED IMAGE RESULTS

Figure 16 shows the hold from the perspective of the shaded image plots. The features present in the shaded image plots are pointed out in Figure 16. The primary features are the king post, the calorimeter, and the furnace.

Figure 18 presents a shaded image temperature plot and air flow vector plot of the four nozzle case at 60 minutes. The forward bulkhead hot spot can be seen at the far left of the figure next to the king post. A second hot spot exists further away from the king post. The temperature mapping displays the hottest region of the calorimeter, which, again, is the cylindrical object near the middle of the figure. Two of the recirculation cells that occurred in the two nozzle case also occurred in the four nozzle case. The recirculation cell in front of the furnace near the overhead is larger than the corresponding recirculation cell in the two nozzle case. The recirculation cell that was in front of the furnace and near the deck in the two nozzle case has moved forward and has reduced in size. The recirculation cell that was near the front bulkhead in the two nozzle case has disappeared and another recirculation cell has formed directly in front of the calo-

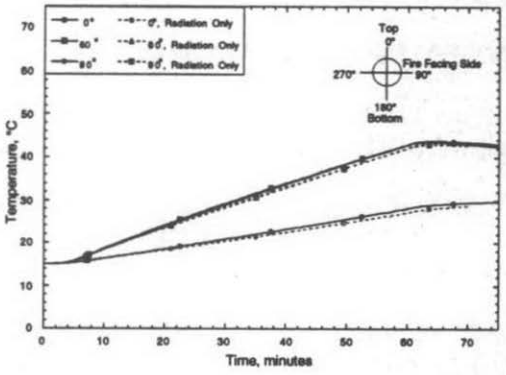

Figure 15 - Comparison of the calorimeter surface temperature with and without convection and fluid conduction

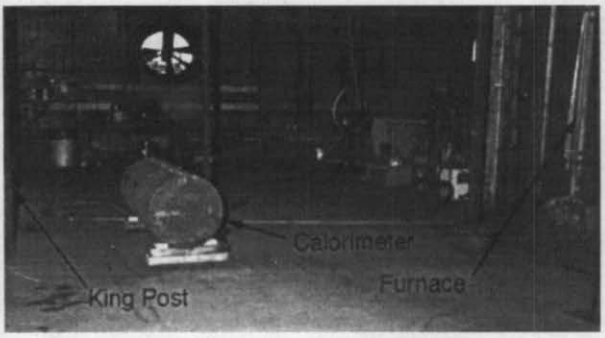

Figure 16 - Ship Hold Test Layout

rimeter and is smaller than the recirculation cell near the front bulkhead in the two nozzle case.

Upward flow occurs near the front bulkhead and above the calorimeter. Flow also occurs under the calorimeter. Upward flow was also evident in the experimental data. A series of flow visualization devices were constructed directly above the calorimeter. Review of videotape taken during the tests show the upward flow from the flow visualization devices.

CONCLUSIONS

The temperature and heat flux values calculated in this analysis are comparable to what was observed from tests. The reasonable calculated temperature and heat flux values indicated that the thermal response of a ship hold with an adjacent hold fire can be predicted.

The calculated circumferential temperature and heat flux patterns were similar to the experimental results. The patterns build confidence that a ship hold thermal response can be successfully modeled.

The model also shows that the predominant mode of heat transfer in this case is radiation. The large time scale for heating components also indicates that radiation is the dominant heat transfer mechanism. However, convection is present and can be a larger factor in transferring heat in other cases.

REFERENCES

CFX-F3D Users Manual, Version 4.1, AEA Technologies, Pittsburg, PA, October, 1995

B.F. Blackwell et al., A Users Manual for the Sandia One-Dimensional Direct and Inverse Thermal (SODDIT) Code, SAND85-2478, Sandia National Laboratories, May, 1987

J.A.Koski et al., Experimental Determination of the Shipboard Fire Environment for Simulated Radioactive Material Packages, SAND97-0506, Sandia National Laboratories, Albuquerque, NM March 1997

J.A. Koski et al., Calculation of Shipboard Fire Conditions for Radioactive Materials Packages with the Methods of Computational Fluid Dynamics, SAND97-2182, Sandia National Laboratories, Albuquerque, NM March 1997

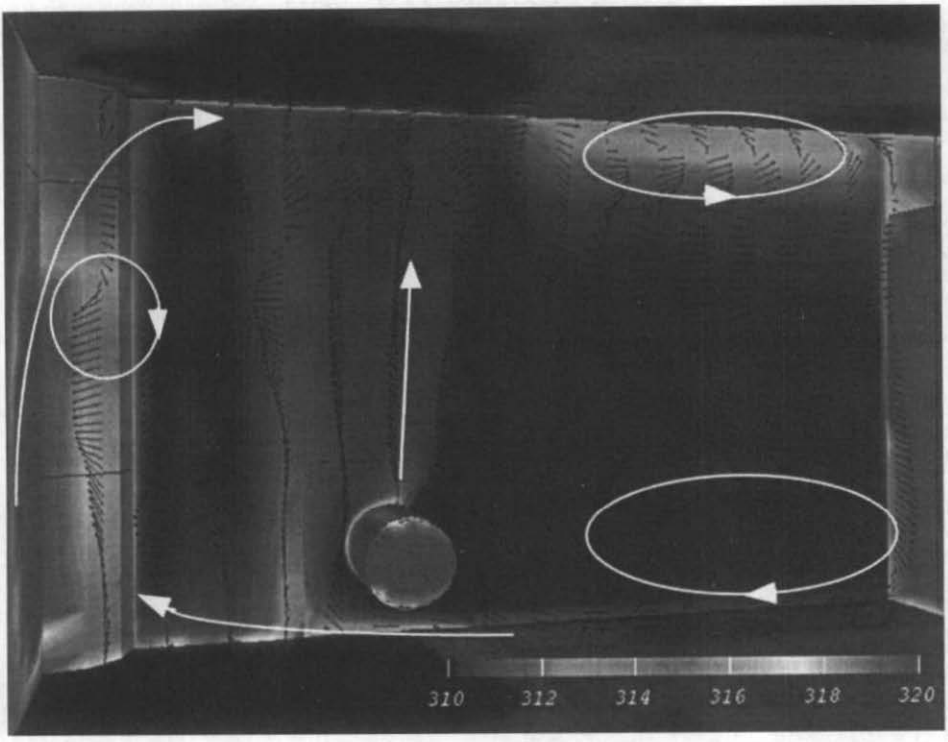

Figure 18 - Four nozzle temperature and air flow vector plot at 60 minutes